

Photocatalytic decomposition of aspartic acid over bare and silver deposited TiO₂

Erzsébet Szabó-Bárdos, Erika Pétervári, Viktória El-Zein, Attila Horváth*

Department of General and Inorganic Chemistry, University of Veszprém, P.O. Box, 158, H-8201 Veszprém, Hungary

Received 6 January 2006; received in revised form 14 April 2006; accepted 20 April 2006

Available online 28 April 2006

Abstract

Photodegradation of aspartic acid over UV irradiated bare and silver deposited titanium dioxide was investigated. It has been demonstrated that the nitrogen content of the amino acid is converted dominantly into NH₃ (detected as NH₄⁺). The evolution of CO₂ was also measured. Both of these processes resulted in a considerable increase of pH in the liquid phase of the reaction mixture providing significant change in the reaction mechanism. Under prolonged irradiation NH₄⁺ is oxidized through NO₂⁻ intermediate to NO₃⁻. The primary steps of the mechanism of photodegradation are analyzed and described considering the results of competitive kinetic studies performed by using oxalic acid as efficient hole scavenger, coumarin as •OH scavenger and various bare and silver deposited titanium dioxide.

© 2006 Elsevier B.V. All rights reserved.

Keywords: Photodegradation; Photocatalysis; Titanium dioxide; Aspartic acid; Oxalic acid; Coumarin

1. Introduction

Photodegradation and mineralization of organic and inorganic pollutants on semiconductor particles have been extensively studied. Biochemical application of TiO₂ mediated photocatalysis are also promising. In this respect systematic studies on photooxidation of amino acids as building blocks of proteins are particularly important. Decomposition of a series of amino acids in aqueous titania dispersions under illumination with UV-A and UV-B was carefully studied and the formation of NH₄⁺, NO₃⁻ and CO₂ was reported by Hidaka et al. [1]. The ratios of evolved nitrogen containing products (NH₄⁺, NO₃⁻) and the rate constants of the formation of these species and that of CO₂ were compared. The mechanistic features were also discussed in this article and it had been concluded that the formation of NH₃ implicated both TiO₂ surface electrons and surface •OH radicals while the reaction with •OH, HO₂• radicals lead to formation of CO₂ in various pathways. A more detailed study focussed to the photooxidation of L-aniline, L-serine and L-phenylalanine and involved molecular orbital calculations has confirmed the proposed mechanism [2].

To reveal the mechanism of photomineralization of a substrate by semiconductor photocatalyst determination of the yield of surface electrons and holes and indication of radical species formed by primary electron transfer are of paramount importance. Various methods (e.g. ESR spectroscopy [3–5], photoluminescent [6–8] and chemiluminescent [9] probing) have been developed for detection of the reactive species containing oxygen such as •OH, HO₂•, ¹O₂, H₂O₂. The use of coumarin or terephthalic acid to measure •OH production in TiO₂ photocatalysis has been reported recently [6,7]. Silver deposition on TiO₂ surface was demonstrated to enhance the photocatalytic degradation of various organic compounds such as phenol, 2-chlorophenol, sucrose, methyl orange, oxalic acid, etc. [10–16]. In a recent study photomineralization rates for a series of carefully selected organic compounds using bare and on silver deposited TiO₂ were measured and analyzed. It has been concluded that the presence of silver on the TiO₂ surface mainly enhances the photocatalytic oxidation of organic compounds that are predominantly oxidized by holes while has only insignificant effect on those organic materials which require •OH radicals for their decomposition [17]. So silver deposition can be applied as a useful tool not only to increase the efficiency of photomineralization but also to provide additional information on revealing the mechanism of the semiconductor mediated photocatalytic processes. Oxalic acid is readily photooxidized

* Corresponding author. Tel.: +36 88 624 341; fax: +36 88 624 548.
E-mail address: attila@vegic.vein.hu (A. Horváth).

over TiO_2 and the reaction rate is significantly increased by silver deposition [14]. It confirms that oxalic acid is a typical hole scavenger. Hence it is reasonable to assume that applying silver deposition with oxalic acid as hole scavenger and with coumarin as $\bullet\text{OH}$ scavenger our knowledge on the role of surface electrons, holes and hydroxyl radicals in the mineralization of a given organic compound can be considerably deepen.

In the present paper, the results obtained by photodecomposition of aspartic acid over various type of TiO_2 are demonstrated. The mechanistic aspects of photoinduced processes are discussed by considering the results of experiments utilized the advantageous of silver deposition on TiO_2 providing efficient charge separation at the surface of semiconductor particle and used oxalic acid and coumarin as scavenger for hole and hydroxyl radical, respectively.

2. Experimental

2.1. Materials

The titanium dioxide samples used in experiments were Degussa P25 (70% anatase, 30% rutile; with a surface area of $50 \text{ m}^2 \text{ g}^{-1}$), Aldrich TiO_2 (mainly anatase, with a surface area of $9.6 \text{ m}^2 \text{ g}^{-1}$) and Fluka TiO_2 (mainly rutile, with a surface area of $9.7 \text{ m}^2 \text{ g}^{-1}$).

For preparing silver deposited TiO_2 solutions of $[\text{Ag}^+] = 10^{-4} \text{ M}$ were prepared by Ag_2SO_4 and AgNO_3 (Reanal) of pure reagent grade. Other reagents, such as oxalic acid, aspartic acid, KMnO_4 , $\text{Ba}(\text{OH})_2$, fluorescamine, coumarin and 7-hydroxycoumarin were purchased from Reanal. The initial pH of the reaction mixture was adjusted using H_2SO_4 and NaOH of pure reagent grade. The high purity water used in the experiments was double distilled and then purified with the Milli-Q system.

2.2. Photocatalytic experiments

Photochemical experiments were performed using a large scale ($\sim 3 \text{ dm}^3$) reactor developed in our laboratory for irradiation of heterogeneous reaction mixture circulated by continuously fed air with a flow rate of $40 \text{ dm}^3 \text{ h}^{-1}$ and described in a previous paper [14]. The photon flux of the internal light source (40 W, $\lambda_{\text{max}} = 350 \text{ nm}$) was determined by tris(oxalato)ferrate(III) chemical actinometer. The initial volume of the reaction mixture was 3 dm^3 in all photochemical experiments in which the concentration of TiO_2 was 1 g dm^3 . The initial concentration of aspartic and oxalic acid was adjusted to be 10^{-3} M . Silver deposited TiO_2 was prepared by photolysis of AgNO_3 or Ag_2SO_4 prior to use it as photocatalyst for degradation of aspartic acid. The initial concentration of Ag^+ was adjusted to be 10^{-4} M . The photodeposition of the noble metal was completed within 40 min, which was checked by the analytical procedure performed on an aliquot sample of the reaction mixture as given elsewhere [14].

2.3. Analytical procedures

Before and after irradiation 4 cm^3 samples were taken from the reactor through the septum with a syringe. The solid phase of sample was separated by filtration using Millipore Millex-LCR PTFE $0.45 \mu\text{m}$. The concentration of the oxalic acid was determined by classical permanganometry using the aliquot of the clear liquid sample. It should be noted that organic compounds such as aspartic acid can also oxidized by MnO_4^- . Therefore, as a preliminary experiment samples prepared by using various ratios of oxalic and aspartic acid stock solutions, respectively, were titrated by KMnO_4 solution in the same conditions as used for the experiments. This measurements indicated a negligible influence of aspartic acid. The concentration of amine function of aspartic acid was determined by fluorescamin [2]. The aliquot sample ($100 \mu\text{l}$) was added to $500 \mu\text{l}$ fluorescamin solution, then using $500 \mu\text{l}$ borate buffer ($0.04 \text{ M H}_3\text{BO}_3$, 0.04 M NaOH , 0.04 M KCl) and water of high purity the solution was diluted to 5 ml. The luminescence spectra of this solution (peaking at 480 nm ; $\lambda_{\text{exc}} = 393 \text{ nm}$) were measured by a Perkin-Elmer LS 50 B fluorimeter. The emission spectra of 7-hydroxycoumarin, in various concentrations of the pure compound for calibration and that of the formed in the reaction of coumarin and hydroxyl radical produced by photolysis, were also detected by Perkin-Elmer LS50B fluorimeter. The concentration of nitrate ions was measured by spectrophotometric method using 2,6-dimethylphenyl reagent in acidic conditions (H_2SO_4). The analytical measuring curve was obtained by using standard KNO_3 solutions in the same conditions. CO_2 evolved and transported by the continuously fed air was absorbed in saturated $\text{Ba}(\text{OH})_2$ solution. To obtain complete absorption of CO_2 two parallel series of absorbers consisting of three units were used. The air flowing out from the reactor was alternately passed through one of this series of absorbers using a three-position tap set between the reactor and absorbers. The BaCO_3 precipitate formed under a given period of the irradiation was separated by filtration and measured according to the gravimetric procedure.

3. Results and discussion

3.1. Photoconversion of aspartic acid on bare TiO_2

Adsorption of aspartic acid on the surface of TiO_2 particles either in dark or under UV excitation strongly depends on pH measured in aqueous phase of the reaction mixture as well as on the nature of TiO_2 particles. The pH determines the charge at the catalyst's surface and the mole fractions of various forms of aspartic acid: $\text{COOHCH}_2\text{CH}(\text{NH}_3^+)\text{COOH}$ (HAsp^+), $\text{COOHCH}_2\text{CH}(\text{NH}_3^+)\text{COO}^-$ ($\text{Asp}^{\text{zwitter}}$), $\text{COO}^- \text{CH}_2\text{CH}(\text{NH}_3)\text{COO}^-$ (Asp^-), and $\text{COO}^- \text{CH}_2\text{CH}(\text{NH}_2)\text{COO}^-$ (Asp^{2-}) in the bulk of aqueous phase. The nature of catalyst involves the crystalline structure, the specific surface area, the average size and size distribution of semiconductor particles. A small but significant differences between the amount of aspartic acid adsorbed on the surfaces of various type of photocatalysts used in present work were observed in dark (before illumination). The Degussa P25

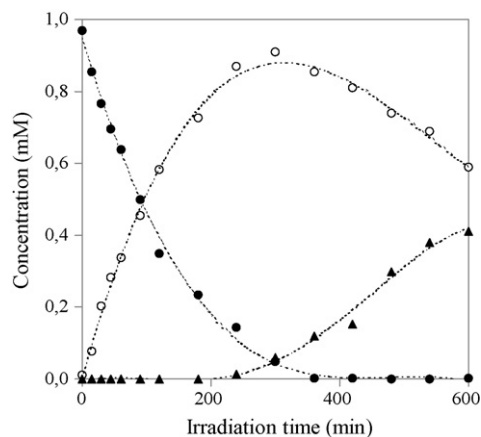


Fig. 1. Disappearance of the primary amine and the concentration of the formed ammonia (NH_4^+) and nitrate ion (NO_3^-) during the course of the photomineralization of aspartic acid over Degussa P25 TiO_2 . The dashed and continuous lines are obtained by polynomial fitting to get the initial rate of the disappearance of amine function ($6.6 \times 10^{-6} \text{ M min}^{-1}$) and that of the formation of ammonium ion ($6.5 \times 10^{-6} \text{ M min}^{-1}$) and nitrate ion.

adsorbs nearly 5% of the aspartic acid of 10^{-3} M at $\text{pH} \sim 3.5$, where its dominant form is the zwitter ion (Asp). The Fluka TiO_2 , which is rutile, and the commercial product of Aldrich particles (anatase) adsorb about 2–3% of the acid in the same conditions.

The disappearance of the amine function of aspartic acid and the temporal evolution of ammonium and nitrate ions under photolysis are demonstrated in Fig. 1. The initial rate of these processes are the same within the experimental error ($6.6 \times 10^{-6} \pm 10^{-7} \text{ M}^{-1} \text{ min}^{-1}$ for disappearance of amine function and $6.5 \times 10^{-6} \pm 10^{-7} \text{ M}^{-1} \text{ min}^{-1}$ for ammonium ion formation). The maximum in the concentration of ammonium ion is observed at 300 min irradiation when the conversion of amino acid approaches to 95%. Nitrate ions are observed after 200 min photolysis and then their concentration increases. It should be noted that NO_2^- ions were also detected under irradiation; however, the highest concentration of this species was about 10^{-6} M (at 350 min irradiation). The nitrogen balances calculated by using concentrations measured for aspartic acid and the nitrogen containing intermediates of measurable (NH_4^+) and detectable amount (NO_2^-) and the final product (NO_3^-) were between 95 and 101%. These results indicate that most of the nitrogen containing species were detected during the experiments. It is also important to note that the loss of the primary amine function of aspartic acid is considerably slowing down over 200 min irradiation and the formation rate of NO_3^- is comparable with that of the disappearance of ammonia over 300 min irradiation.

Fig. 2 shows the increase of evolved CO_2 and the change of the pH in the aqueous phase under irradiation. The dashed line shows the amount of CO_2 expected if the loss of primary amine would be the rate determining step of the complete photodegradation. The pH increases slowly than rapidly and finally it levels off. The shape of the pH change is very similar to that of measured for CO_2 evolution. The measured and the “expected” CO_2 data coincide in the final period of the irra-

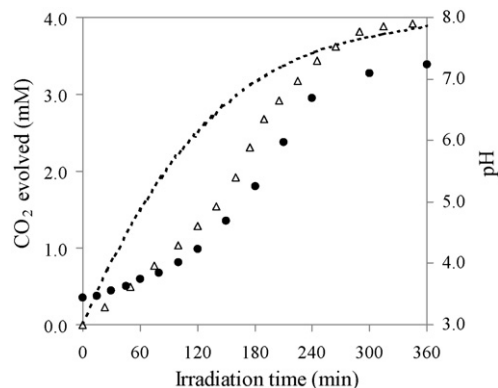


Fig. 2. Formation of CO_2 (Δ) and the change of pH (\bullet) during the course of photomineralization of aspartic acid. The dark dashed line indicate the theoretically estimated CO_2 evolution obtained by supposing a very rapid and complete oxidation of the radical formed by loss of amine function. The initial rate of CO_2 formation obtained by polynomial fitting (gray dashed line) is $1.13 \times 10^{-5} \text{ M min}^{-1}$.

diation. These observations indicate a change in the mechanism of the photomineralization. The increase in pH, due to the release of ammonia and oxidation of carboxylic groups, leads to significant effects, namely (1) the deprotonation of Asp, (2) the change in the surface charge from positive to negative at the isoelectric point of the titania, which accompanies with (3) the shift in both the valence and conduction band energy level of UV excited titania to more reducing potentials [18]. The first results in a considerable decrease in the rate of electron scavenging by the aspartic acid [19]. The second should decrease the adsorption of the anionic form of the amino acid due to the negative charge of the aspartate. The third influences the driving force of the primary electron transfer reactions of the excited TiO_2 . Hence the efficiency of electron attack on amino group decreases with increasing pH, and most of the surface electrons are scavenged by O_2 that provides the predominance of the oxidizing radicals over the excited semiconductor particles resulting in an increase in the rate of CO_2 evolution.

Fig. 3 demonstrates the decrease in the concentration of aspartic acid within the aqueous phase under photolysis using various

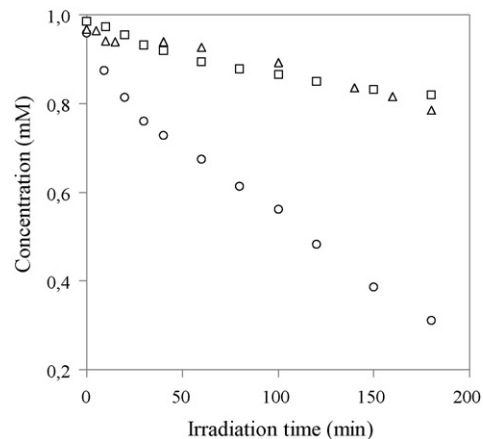


Fig. 3. Disappearance of the primary amine function during the course of the photomineralization of aspartic acid over Degussa P25 (\circ), Fluka (\square) and Aldrich (Δ) TiO_2 .

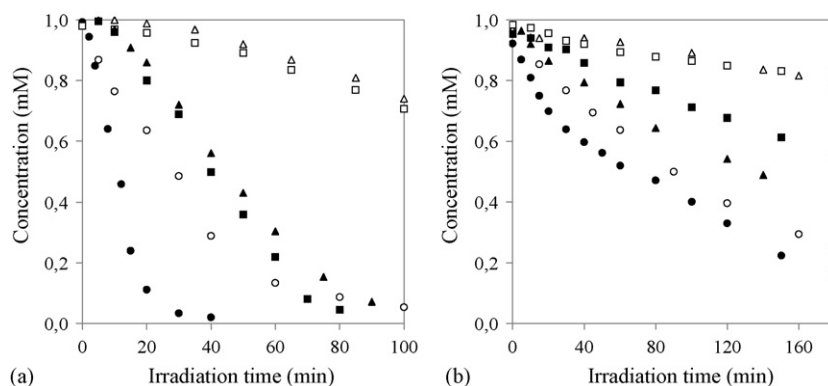


Fig. 4. Photodegradation of oxalic acid (a) and aspartic acid (b) over various TiO_2 : (○) bare Degussa P25, (●) Ag deposited Degussa P25, (□) bare Fluka, (■) Ag deposited Fluka, (△) bare Aldrich, (▲) Ag deposited Aldrich.

titania. The irradiation over a period of 200 min leads to nearly 80% decomposition over P25 photocatalyst, while the reaction occurs slowly when rutile or anatase is used.

3.2. Photoconversion of aspartic acid enhanced by silver modified catalysts

The effects of silver deposition on the efficiency of the photocatalysts in the mineralization of aspartic acid and oxalic acid have been compared. It should be emphasized that the latter compound is known as typical hole scavenger [14,17]. Fig. 4 shows the decrease in the concentration of the reactants under photolysis over three different titania. A considerable enhancement in the rate of photoreaction on each silver deposited catalyst is observed for oxalic acid. On the other hand the influence of silver deposition in the initial rate of photodecomposition of aspartic acid using Degussa P25 is rather small. Comparing these findings with the ascertainment of Tran et al. [17] whereas “the presence of silver mainly enhances the photocatalytic oxidation of organic compounds that are predominantly oxidized by holes”, it is confirmed that the loss of amine function of aspartic acid does not directly initiated by photogenerated hole. However, it is also clearly indicated by Fig. 4b that the rate of photooxidation of aspartic acid is significantly increased by silver deposition on Fluka (rutile) and especially on Aldrich catalyst (anatase).

These results suggest that the enhancement in the photoreaction yield caused by silver deposition also depends on the nature (crystal structure, specific surface area, particle size and size distribution) of the semiconductor.

To obtain further information on the effect of the photo-deposited silver the formation of $\bullet\text{OH}$ radical over the photoexcited bare and silver modified titania has been investigated and compared. In these experiments coumarin and oxygen were used as scavengers for $\bullet\text{OH}$ radical [7,8] and electron, respectively. The results illustrated by Fig. 5 show that among the investigated bare titania it is the Aldrich catalyst that has the smallest activity in this regard. On the other hand, the silver deposited form of this catalyst produces most efficiently the hydroxyl radicals as demonstrated by the quantum yield data summarized in Table 1.

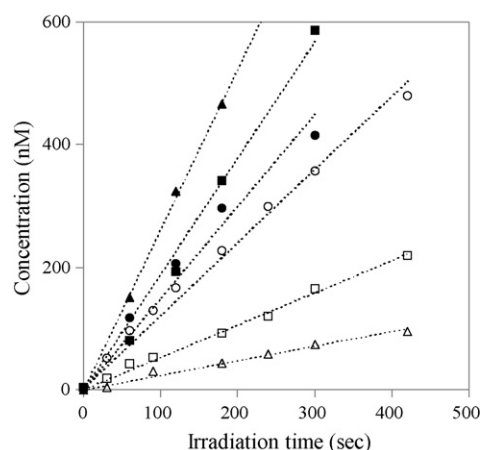


Fig. 5. Formation of 7-hydroxy coumarin under photolysis of coumarin over various TiO_2 : (○) bare Degussa P25, (●) Ag deposited Degussa P25, (□) bare Fluka, (■) Ag deposited Fluka, (△) bare Aldrich, (▲) Ag deposited Aldrich.

These data suggest that the silver deposit on TiO_2 surface provides a better separation of the $\{e^-;h^+\}$ because the silver clusters acts as electron traps. Thus the electron transfer from water to hole competes with the $\{e^-;h^+\}$ recombination more effectively using catalyst modified by silver deposit than the bare titania.

3.3. Competitive photoconversion of aspartic acid and oxalic acid over bare and silver deposited titanium dioxides

To obtain further insight into photodegradation mechanism a series of competitive kinetic experiment using efficient hole

Table 1
Quantum yield of hydroxyl radical scavenging obtained by UV excitation of TiO_2 catalysts using coumarin as radical scavenger

Catalyst	Quantum yield of hydroxyl radical scavenging, Φ		$\Phi(\text{TiO}_2\text{-Ag})/\Phi(\text{TiO}_2)$
	$\Phi(\text{TiO}_2)$	$\Phi(\text{TiO}_2\text{-Ag})$	
Degussa P25	$(2.3 \pm 0.1) \times 10^{-4}$	$(3.1 \pm 0.1) \times 10^{-4}$	1.4
Fluka	$(8.5 \pm 0.2) \times 10^{-5}$	$(3.9 \pm 0.1) \times 10^{-4}$	4.6
Aldrich	$(3.9 \pm 0.1) \times 10^{-5}$	$(5.4 \pm 0.1) \times 10^{-4}$	14.0

The initial concentration of coumarin was 10^{-4} M.

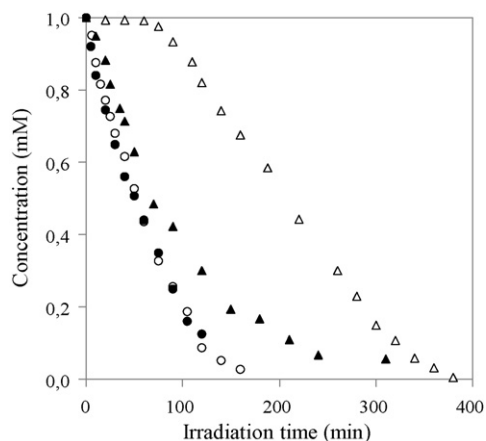


Fig. 6. Competitive photodegradation of aspartic acid and oxalic acids over Degussa P25 photocatalyst: (○) oxalic acid over bare TiO₂, (●) oxalic acid over Ag deposited TiO₂, (Δ) aspartic acid over bare TiO₂, (▲) aspartic acid over Ag deposited TiO₂.

scavengers to minimize the probability of hydroxyl radical formation have been completed. In these experiments oxalic acid was the hole scavenger. A mixture of aspartic acid and oxalic acid have been illuminated over various bare and silver modified titania. The results are demonstrated by Figs. 6–8. The oxalic acid almost completely prevents the aspartic acid from the photodegradation over bare catalysts, and the loss of amin function of Asp starts after the concentration of the oxalic acid is significantly decreased, which is accompanied by the increase of pH. On the other hand, the photooxidation of oxalic acid is also significantly slowed down in the presence of aspartic acid. This mutual inhibition effect suggests an efficient reaction between the radicals formed by primary electron transfer reaction from the surface bonded oxalic acid to hole and the electron transfer from CB to the aspartic acid, respectively. Some of the early steps of the proposed photodegradation mechanism of aspartic acid and oxalic acids are illustrated in Scheme 1, which is divided into two parts to highlight the difference between the events followed by illumination of a bare (a) and that of silver modified (b)

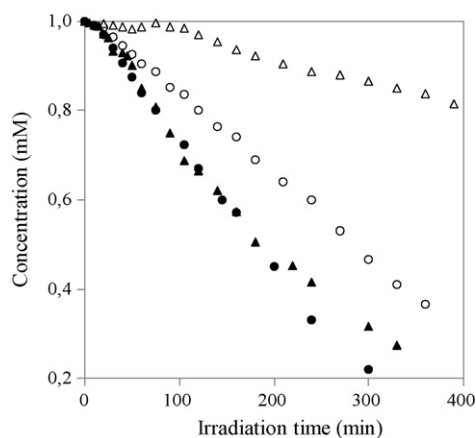


Fig. 7. Competitive photodegradation of aspartic acid and oxalic acids over Fluka photocatalyst: (○) oxalic acid over bare TiO₂, (●) oxalic acid over Ag deposited TiO₂, (Δ) aspartic acid over bare TiO₂, (▲) aspartic acid over Ag deposited TiO₂.

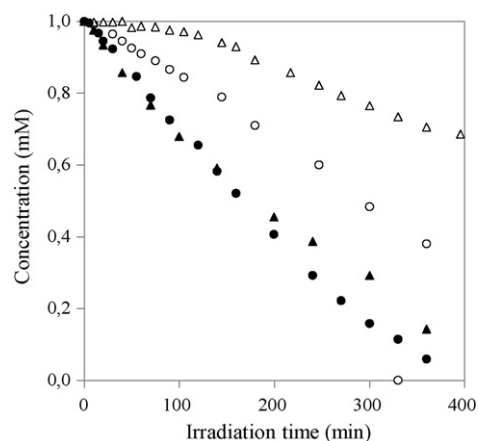


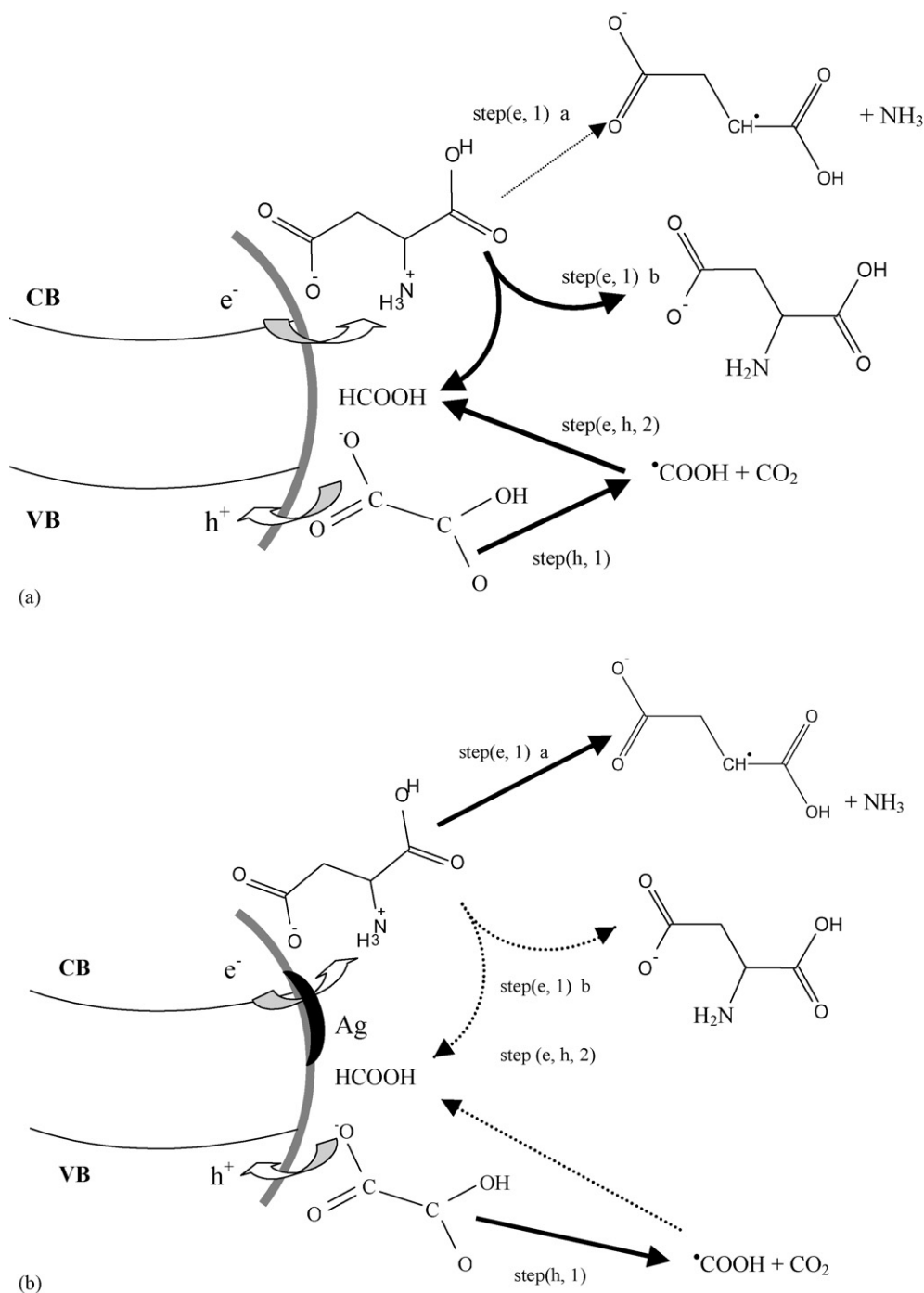
Fig. 8. Competitive photodegradation of aspartic acid and oxalic acids over Aldrich photocatalyst: (○) oxalic acid over bare TiO₂, (●) oxalic acid over Ag deposited TiO₂, (Δ) aspartic acid over bare TiO₂, (▲) aspartic acid over Ag deposited TiO₂.

semiconductor particle. Upon irradiation of the TiO₂ electron is promoted from the VB to CB. The migration of these charge carriers to the particle surface takes place in competition with other trapping and recombination events in the bulk of particle. At the surface of bare TiO₂ are poised to carry out redox reactions with suitable electron acceptors and donors, respectively, in competition with radiative and nonradiative recombinations.

Considering the possible electron scavengers (O₂, H⁺, HAsp⁺ and Asp) and the rate coefficients of their reaction with electron [20] it has been concluded that the zwitter ionic form of the surface bounded aspartic acid efficiently accepts electron resulting in HAsp[•] or Asp^{•-}, while oxalate ion readily transfer electron to the hole producing CO₂ and [•]COOH radical. This radical can abstract electron from HAsp[•] or Asp^{•-} preserving the degradation of the aspartic acid (Scheme 1a). It has been found that among the C₁–C₅ linear carboxylic acids formic acid has the highest rate of photodegradation over TiO₂ [21], so formic acid formed in this system is readily oxidized to CO₂. It is also important to note that formate has been proved to be more efficient electron donor than oxalate in reductive deposition of copper(II) ions over photoexcited titanium dioxide [22], hence formic acid or formate ion should be an intermediate of low concentration under continuous photolysis.

The silver deposition on Degussa P25 does not result in significant increase in the photooxidation rate of oxalic acid while it considerably reduces the inhibition effect of oxalic acid on the disappearance of the amine function of aspartic acid. Silver particles on semiconductor surface trap the electrons and the electron transfer occurs from this level (which is lower than the CB of the bare TiO₂) to HAsp⁺ or Asp. The oxalate, as a sacrificial electron donor transfers electron to the hole producing [•]COOH radical. However, as the surface electrons are trapped by silver cluster and hence are separated from the holes the products of primary electron transfer steps, HAsp[•] or Asp^{•-} and [•]COOH are also separated.

Thus the release of NH₃ follows before the [•]COOH could abstract electron from HAsp[•] or Asp^{•-} (Scheme 1b) and then [•]COOH radical reacts with molecular oxygen producing HO₂[•]



Scheme 1. (a and b) View of primary and secondary steps of simultaneous photoinduced degradation of aspartic acid and oxalic acid initiated by excited TiO_2 particles; bold arrows show the dominant steps while dashed arrows show the steps of low efficiency.

and CO_2 as given elsewhere [14]. The radical formed by release of ammonia ($\text{HOOCCH}_2\cdot\text{CHCOOH}$ or $^-\text{OOCCH}_2\cdot\text{CHCOOH}$) can react with $\text{HO}_2\cdot$ producing a peroxide species that ultimately undergoes further oxidation to yield CO_2 .

4. Conclusions

Photodegradation of aspartic acid has been investigated using various bare and silver deposited TiO_2 photocatalyst and various

scavengers for hole and hydroxyl radical, respectively. The photomineralization was followed by conversion of amine group to NH_4^+ and by evolution of CO_2 . It has been demonstrated that silver deposition on TiO_2 particles results in an increase on photodegradation rate. The most efficient enhancement due to the silver deposition has been observed for anatase (Aldrich TiO_2).

Competitive kinetic studies have been performed using various bare and silver modified titanium dioxide and oxalic acid as efficient hole scavenger. These studies have clearly indicated

that the photodecomposition of aspartic acid over bare TiO₂ particles is inhibited by oxalic acid. This finding is explained by a mechanism in which the key reaction step is a hydrogen abstraction of [•]COOH radical from HAsp[•]. Both of these radicals are formed by the primary electron transfer reactions at the surface of semiconductor particle, namely, by the electron transfer from oxalic acid to the hole and the electron transfer from CB of excited TiO₂ to HAsp⁺, respectively. The silver clusters deposited on the semiconductor surface resulting in an efficient charge separation providing a relatively large distance between the primary radicals, hence a considerable decrease in the efficiency of their reaction. In addition, it is assumed that silver cluster promotes the release of ammonia from HAsp[•] radical.

This contribution provides evidence that combination of the silver deposition with using suitable hole scavenger can be applied as an efficient tool for deepening our knowledge on the elementary reaction steps occurring over the surface of the photoexcited semiconductor particles.

References

- [1] H. Hidaka, S. Hirokoshi, K. Ajisaka, J. Zhao, N. Serpone, J. Photochem. Photobiol. A Chem. 108 (1997) 197–205.
- [2] S. Horikoshi, N. Serpone, J. Zhao, H. Hidaka, J. Photochem. Photobiol. A Chem. 118 (1998) 123–129.
- [3] D. Dvoranova, V. Brezová, M. Mazúr, M.A. Malati, Appl. Catal. B Environ. 37 (2002) 91–95.
- [4] V. Brezová, P. Trábek, D. Dvoranová, A. Staško, S. Biskupič, J. Photochem. Photobiol. A Chem. 155 (2003) 179–198.
- [5] V. Brezová, S. Gabčová, D. Dvoranová, A. Staško, J. Photochem. Photobiol. B Biol. 79 (2005) 121–134.
- [6] K. Ishibasi, A. Fujishima, T. Watanabe, K. Hashimoto, J. Photochem. Photobiol. A Chem. 134 (2000) 139–142.
- [7] K. Ishibasi, A. Fujishima, T. Watanabe, K. Hashimoto, Electrochem. Commun. 2 (2000) 207–210.
- [8] Y. Nosaka, T. Daimon, A.Y. Nosaka, Y. Murakami, Phys. Chem. Chem. Phys. 6 (11) (2004) 2917–2918.
- [9] D. Chatterjee, A. Mahata, J. Photochem. Photobiol. A Chem. 154 (2003) 19–23.
- [10] D. Schukin, E. Ustinovich, D. Sviridov, P. Pichat, Photochem. Photobiol. Sci. 3 (2004) 142–144.
- [11] V. Vamathevan, R. Amal, D. Beydoun, G. Low, S. McEvoy, J. Photochem. Photobiol. A Chem. 148 (2002) 233–245.
- [12] I.M. Arbatzis, T. Streigopoulos, M.C. Bernard, D. Labou, S.G. Neophytides, Appl. Catal. B 42 (2003) 187–201.
- [13] M. Sokmen, D.W. Allen, F. Akkas, N. Kartal, F. Acar, Water Air Soil Pollut. 132 (2001) 153–163.
- [14] E. Szabó-Bárdos, H. Czili, A. Horváth, J. Photochem. Photobiol. A Chem. 165 (2004) 195–201.
- [15] W. Lee, H.S. Shen, K. Dwight, A. Wold, Chem. Eng. J. 98 (2004) 127–139.
- [16] M. Moonsiri, P. Rangsunvigit, S. Chavadej, E. Gulari, Chem. Eng. J. 97 (2004) 241–248.
- [17] H. Tran, K. Chiang, J. Scott, R. Amal, Photochem. Photobiol. Sci. 4 (2005) 565–567.
- [18] H.O. Finklea, Semiconductor Electrodes, Elsevier, Amsterdam, 1988.
- [19] The deprotonation of amino and then the carboxylic group results in significant decrease in the rate coefficient of electron scavenging, namely $k = 6 \times 10^9 \text{ M}^{-1} \text{ s}^{-1}$ for $\text{e}^-_{\text{aq}} + \text{Asp}^+$, $k = 6 \times 10^8 \text{ M}^{-1} \text{ s}^{-1}$ for $\text{e}^-_{\text{aq}} + \text{Asp}$, and $k = 1.8 \times 10^7 \text{ M}^{-1} \text{ s}^{-1}$ for $\text{e}^-_{\text{aq}} + \text{Asp}^-$ as given in [20].
- [20] G.V. Buxton, C.L. Greenstock, W.P. Helman, A.B. Ross, J. Phys. Chem. Ref. Data 17 (2) (1988) 513–886.
- [21] N. Serpone, J. Martin, S. Horikoshi, H. Hidaka, J. Photochem. Photobiol. A Chem. 169 (2004) 234–250.
- [22] S. Yamazaki, S. Iwai, J. Yano, H. Taniguchi, J. Phys. Chem. A 105 (2001) 11285–11290.